PHYSICAL REVIEW D **83,** 083521 (2011)

Constraints on the induced gravitational wave background from primordial black holes

Edgar Bugaev* and Peter Klimai†

Institute for Nuclear Research, Russian Academy of Sciences, 60th October Anniversary Prospect 7a, 117312 Moscow, Russia

(Received 21 December 2010; published 25 April 2011)

We perform a consistent calculation of primordial black hole (PBH) mass spectrum and second-order induced gravitational wave (GW) background produced from primordial scalar perturbations in radiation era of the early Universe. It is shown that the maximal amplitudes of the second-order GW spectrum that can be approached without conflicting with the PBH data do not depend significantly on the shape of primordial perturbation spectrum. The constraints on the GW background obtained in previous works are extended to a wider GW frequency range. We discuss the applicability of the currently available pulsar timing limits for obtaining the constraints on scalar power spectrum and PBH abundance and show that they can be used for strongly constraining the PBH number density in the PBH mass range $\sim(0.03 - 10)M_{\odot}$.

DOI: 10.1103/PhysRevD.83.083521 PACS numbers: 98.80.−k, 04.30.Db

I. INTRODUCTION

It is well known now that gravitational waves (GWs) can be effectively generated by density perturbations during the radiation dominated era. Tensor and scalar perturbations are decoupled at the first order, but it is not so in higher orders of cosmological perturbation theory. Namely, the primordial density perturbations and the associated scalar metric perturbations generate a cosmological background of GWs at second order through a coupling of modes [1–3]. In particular, a second-order contribution to the tensor mode, $h_{ij}^{(2)}$, depends quadratically on the first-order scalar metric perturbation, i.e., the observed scalar spectrum sources the generation of secondary tensor modes. By other words, the stochastic spectrum of second-order GWs is induced by the first-order scalar perturbations. Calculations of Ω_{GW} at second order and discussions on perspectives of measurements of the second-order GWs are contained in works [4–9].

It is natural to conjecture that the detection of GWs from primordial density perturbations on small scales (not directly probed by observations) could be used to constrain overdensities on these scales, in a close analogy with the case of primordial black holes (PBHs). However, at the present time, gravitational wave background (GWB) is not yet detected. So, on the contrary, one can constrain GWB using existing limits on amplitudes of primordial density perturbations. Such limits are available, in particular, from studies of primordial black hole production in the radiation era.

It is generally known that PBHs form from the density perturbations, induced by quantum vacuum fluctuations during inflationary expansion. For an efficient production of PBHs in the early Universe [10–13] the spectrum of the density perturbations set down by inflation must be "blue", i.e., it must have more power on small scales. This implies that the spectral index of the scalar perturbations must be larger than 1, in strong contradiction with the latest WMAP results [14–16]. Such a conclusion is correct, however, only in rather special case: namely, it is based on the prediction of slow-roll single-field inflationary scenario, according to which the power spectrum of curvature perturbations is nearly scale-invariant, i.e., the spectral index n is close to unity and the variation in the spectral index $dn/d\log k$ is small.

Although a prediction of the approximate scale invariance of the primordial power spectrum is a necessary requirement to any inflationary model, some deviations from pure scale invariance are consistent with the observational data. These deviations are described by adding localized features to the primordial spectrum (see, e.g., [17] and references therein) and/or by introducing spectral features modifying a single power law. Models with such peculiarities (sometimes called broken-scale-invariant (BSI) models) were proposed, in main aspects, in eighties [18–23]. Such models generally include, in addition to the usual inflaton field, other scalar fields driving successive stages of inflation and triggering phase transitions.

Evidently, the BSI models of inflation could predict, generically, the essential production of primordial black holes at small and medium scales. In particular, second-order phase transitions during inflationary expansion had been first considered in [20,22] in models with two scalar fields. In scenarios of such type, during a short stage, corresponding to the beginning of a phase transition, the mass of the trigger field becomes negative and adiabatic perturbations are exponentially amplified resulting in the formation of a narrow spike in the primordial spectrum and, as a consequence, in a copious production of PBHs [24,25]. There are many multiple field scenarios predicting the existence of spike or bumplike features in the primordial spectrum (e.g., supersymmetric double hybrid models [26], multiple inflation models based on supergravity [27],

*bugaev@pcbai10.inr.ruhep.ru
†pklimai@gmail.com

etc). Some of these models are specially constructed to predict efficient PBH production [28,29].

An existence of the narrow spikes in the primordial spectrum is possible not only in multiple field inflationary scenarios. Such a feature can, in principle, exist even in single-field models (see, e.g., [30,31]). If, e.g., the inflationary potential has an unstable maximum at origin (e.g., the double-well potential) then, with some fine-tuning of parameters and initial conditions, the inflation process may have two stages, with a temporary stay at the maximum, that may lead to the corresponding peak in the primordial spectrum and, depending on the amplitude of the peak, to the PBH production.

The details of the PBH formation from the density perturbations have been studied in [32,33]; the astrophysical and cosmological constraints on the PBH density have been obtained in many subsequent works (see, e.g., the recent reviews [13,34]). The order of magnitude of the corresponding constraint on the value of the density perturbation amplitude is well known [35], but, if the primordial spectrum contains the peaklike feature, the concrete value of the PBH constraint clearly depends on the parameters characterizing the form of this feature (in particular, on the width of the peak). Such an information may be rather useful for the model makers.

The aim of the present work is twofold. In the first part of the work, we obtain constraints on a power spectrum of the primordial fluctuations (for the particular case when the spectrum has a peak feature) for a wide range of PBH masses ($10^9 \div 10^{38}$ g). Recently, the constraints on the curvature perturbation from PBHs had been compiled and updated in Ref. [36]. Authors of [36] assume that the PBHs form at a single epoch and that, over the scales probed by a specific PBH abundance constraint, the curvature power spectrum can be written as a power law (with a spectral index close to 1). In contrast with this, we assume that the curvature perturbation spectrum has a peak, and the position of this peak determines the epoch of the PBH production. A width of this peak is a model parameter, and the peak value is constrained by corresponding data (on nucleosynthesis, photon extragalactic background, cosmological energy density parameter).

In the second part of the work, we use the constraints on the curvature perturbation derived in such a way for constraining the energy density of the induced GW background (different values of PBH masses correspond to different values of a frequency of this background). In our previous work [37] a part of these constraints was obtained for rather narrow range of frequencies ($\sim 10^{-3} \div 10^{3}$ Hz), whereas in this paper we do it for the interval $\sim 10^{-10} \div 10^{4}$ Hz.

The plan of the paper is as follows. In Sec. II, we present the main relations which are necessary for a PBH mass spectrum calculation. In Sec. III, we introduce our parametrization of the power spectrum of primordial curvature perturbations, having a peak feature, and demonstrate a dependence of the PBH mass spectrum on a width of the peak. In Sec. IV, we obtain the constraints on the peak value of the primordial curvature spectrum from nonobservation of PBHs and products of their Hawking evaporation. In Sec. V, we give the main formulas used for the calculation of the induced GWB. Constraints on $\Omega_{\rm GW}$ derived from PBH constraints on the primordial curvature spectrum are presented in Sec. VI. The last Section contains our conclusions and discussions.

II. PBH MASS SPECTRUM CALCULATION

The calculation of PBH mass spectrum in Press-Schechter formalism [38] is based on the expressions [39–41]

$$n_{\rm BH}(M_{\rm BH})dM_{\rm BH} = \left\{\int n(M,\delta_R)\frac{d\delta_R}{d\delta_R^H}\frac{dM}{dM_{\rm BH}}d\delta_R^H\right\}dM_{\rm BH}, \tag{1}$$

$$n(M,\delta_R) = \sqrt{\frac{2}{\pi}}\frac{\rho_i}{M}\frac{1}{\sigma_R^2}\left|\frac{\partial\sigma_R}{\partial M}\left(\frac{\delta_R^2}{\sigma_R^2}-1\right)\right| e^{-(\delta_R^2/2\sigma_R^2)}. \tag{2}$$

Here, the following notations are used: δ_R is the initial (at the moment t_i) density contrast smoothed on the comoving scale R, M is the smoothing mass (initial mass of the fluctuation corresponding to the scale R), $\sigma_R(M)$ is the mean square deviation (the mass variance),

$$\sigma_R^2(M) = \int_0^\infty \mathcal{P}_\delta(k)W^2(kR)\frac{dk}{k}, \tag{3}$$

$\mathcal{P}_\delta(k)$ is the power spectrum of primordial density perturbations, $W(kR)$ is the Fourier transform of the window function (in this work we use the Gaussian one, $W(kR) = \exp(-k^2R^2/2)$), ρ_i is the initial energy density. It is assumed that the process of reheating is very short in time, so the end of inflation practically coincides with a start (at $t = t_i$) of the radiation era.

Fourier transform of the (comoving) density contrast is

$$\delta_k(t) = -\frac{2}{3}\left(\frac{k}{aH}\right)^2\Psi_k(t), \tag{4}$$

where $\Psi_k(t)$ is the Fourier transform of the Bardeen potential. Here, we explicitly take into account the time dependence of the Bardeen potential.

The power spectrum of the density perturbations, calculated at some moment of time, is

$$\mathcal{P}_\delta(k,t) = \left[\frac{2}{3}(k\tau)^2\right]^2\mathcal{P}_\Psi(k,t), \tag{5}$$

where τ is the conformal time ($\tau = (aH)^{-1}$ for the radiation epoch).

The comoving smoothing scale, $R \equiv 1/k_R$, is connected with the smoothing mass M by the expression

$$\left(\frac{M}{M_i}\right)^{-2/3} = \frac{k_R^2}{(a_i H_i)^2}, \tag{6}$$

where M_i, a_i, and H_i are the horizon mass, cosmic scale factor, and Hubble parameter at the moment t_i.

In the approximation of instantaneous transition from inflationary era to the radiation dominated epoch, the connection between density perturbation at any time and curvature perturbation at initial moment of time t_i is [42]

$$\mathcal{P}_\delta(k, t) = \left[\frac{2}{3}(k\tau)^2 \frac{\Psi_k(\tau)}{\mathcal{R}_k(\tau_i)}\right]^2 \mathcal{P}_\mathcal{R}(k, t_i), \tag{7}$$

where the expression for $\Psi_k(\tau)$ is given by [43]

$$\Psi_k(\tau) = \frac{2\mathcal{R}_k(\tau_i)}{x^3}[(x - x_i)\cos(x - x_i) - (1 + x x_i)\sin(x - x_i)],$$
$$x = \frac{k\tau}{\sqrt{3}}, \qquad x_i = \frac{k\tau_i}{\sqrt{3}}. \tag{8}$$

Here, $\mathcal{R}_k(\tau_i)$ is the Fourier component of the curvature perturbation on the comoving hypersurfaces at the end of inflation (see, e.g., [43]).

The connection between values of the smoothing mass M, density contrast δ_R^H, and PBH mass $M_{\rm BH}$ can be expressed in the general form

$$M_{\rm BH} = \varphi(M, \delta_R^H; M_i). \tag{9}$$

The concrete expression for the function φ depends on the model of the gravitational collapse. In the model of the standard spherically-symmetric collapse the connection is quite simple:

$$M_{\rm BH} = (\delta_R^H)^{1/2} M_h. \tag{10}$$

Here, M_h is the horizon mass at the moment of time, $t = t_h$, when regions of the comoving size R and smoothing mass M cross horizon. According to Carr and Hawking [44], $1/3 = \delta_{\rm th} \le \delta_R^H \le 1$. The derivation of Eq. (10) is given in the Appendix of [42]. From (10), using the relation $M_h = M_i^{1/3} M^{2/3}$, one has the expression for the function φ for the Carr-Hawking collapse:

$$\varphi(M, \delta_R^H; M_i) = (\delta_R^H)^{1/2} M^{2/3} M_i^{1/3}. \tag{11}$$

In the picture of the critical collapse [45,46] the corresponding function is

$$\varphi(M, \delta_R^H; M_i) = k_c(\delta_R^H - \delta_c)^{\gamma_c} M^{2/3} M_i^{1/3}, \tag{12}$$

where δ_c, γ_c, and k_c are model parameters. The mass spectrum of PBHs for the critical collapse model has been calculated, e.g., in [42]. It was shown that for the primordial scalar perturbation spectrum with a peak the maximum of PBH mass spectrum is still around the horizon mass corresponding to the maximum in primordial power spectrum, but the PBH mass spectrum also has a "tail" of small masses. In this work, we will use classical collapse model [Eq. (11)]. However, in the end of the paper we will explore the dependence of the results on $\delta_{\rm th}$—the density contrast threshold of PBH formation, which gives the main uncertainty due to the exponential sensitivity of PBH abundance to it.

III. PRIMORDIAL POWER SPECTRUM WITH MAXIMUM

It is convenient to use some kind of parametrization to model the realistic peaked power spectrum of finite width. We use the distribution of the form

$$\lg \mathcal{P}_\mathcal{R}(k) = B + (\lg \mathcal{P}_\mathcal{R}^0 - B)\exp\left[-\frac{(\lg k/k_0)^2}{2\Sigma^2}\right]. \tag{13}$$

Here, $B \approx -8.6$, $\mathcal{P}_\mathcal{R}^0$ characterizes the height of the peak, k_0 is the position of the maximum, and Σ is the peak's width. Parameters of such a distribution have been constrained in the previous work of authors [42] from nonobservation of PBHs and products of their Hawking evaporation (photons and neutrinos).

In many cases limits on PBH abundance have been obtained using the assumption that PBH mass distribution is close to the δ-function form. This does not, however, mean that the original spectrum $\mathcal{P}_\mathcal{R}(k)$ should be very narrow. For example, in the calculation of PBH mass spectra given in Fig. 1, all distributions have a distinct

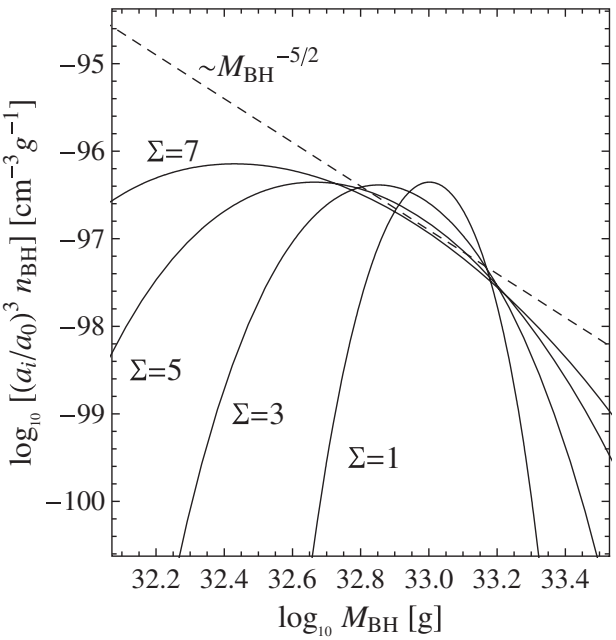

FIG. 1. The calculation of PBH mass spectra for a peaked $\mathcal{P}_\mathcal{R}(k)$ spectrum for $M_h^0 = 10^{33}$ g and different values of Σ. The value of $\mathcal{P}_\mathcal{R}^0$ was chosen so that for all cases $\Omega_{\rm PBH} \approx 0.024$ (for $\Sigma = 1$, $\mathcal{P}_\mathcal{R}^0 = 0.0488$; for $\Sigma = 3$, $\mathcal{P}_\mathcal{R}^0 = 0.0294$; for $\Sigma = 5$, $\mathcal{P}_\mathcal{R}^0 = 0.0267$; for $\Sigma = 7$, $\mathcal{P}_\mathcal{R}^0 = 0.0258$.) The dashed curve shows, for comparison, the form of the classical Carr's $M_{\rm BH}^{-5/2}$-mass spectrum [32].

maximum (even for rather wide peak, $\Sigma = 7$), which shifts to smaller $M_{\rm BH}$ with the growth of Σ. In this sense, if our goal was just to explore the PBH abundance, we could assume that $\mathcal{P}_{\mathcal{R}}(k) \sim \delta(k - k_0)$ from the start, without introducing big mistakes (note, however, that with such an approach the shift of the distribution maximum would not be noticed). This is, however, not an adequate approximation for our study because we are also interested in calculation of the second-order GWB produced by the same power spectrum and studying of its dependence on the width of the peak.

One should note that in Fig. 1 we show on the vertical axis the quantity $n_{\rm BH} \times (a_i/a_0)^3$, which is the physical (rather than comoving) number density of PBHs and is independent on the reheating temperature $T_{\rm RH}$ in the limit $k_i \equiv a_i H_i \gg k_0 = k(M_h^0)$ [42].

The fraction of an energy density of the Universe contained in PBHs today, $\Omega_{\rm PBH}$, assuming that a mass of the produced black hole does not change in time, is

$$\Omega_{\rm PBH} = \frac{1}{\rho_c}\left(\frac{a_i}{a_0}\right)^3 \int M_{\rm BH} n_{\rm BH}(M_{\rm BH}) dM_{\rm BH} \tag{14}$$

(ρ_c is the critical density). This formula is rather accurate for black holes with initial mass $M_{\rm BH} \gg M_*$, where $M_* \approx (3t_0\alpha_0)^{1/3} \approx 5 \times 10^{14}$ g is the initial mass of PBH which reaches its final state of evaporation today [47], $\alpha_0 = 8.42 \times 10^{25}$ g^3 s^{-1}, and t_0 is the age of the Universe.

IV. CONSTRAINTS ON $\mathcal{P}^0_{\mathcal{R}}$

For constraining $\mathcal{P}^0_{\mathcal{R}}$ we use the existing limits on PBH abundance. In the region of $M_{\rm BH}$ which is of interest for us ($10^9 \lesssim M_{\rm BH} \lesssim 10^{38}$ g) these limits can be divided in three groups: i) constraints on PBHs from big bang nucleosynthesis (due to hadron injections by PBHs [48], photodissociation of deuterium [49] and light nuclei, fragmentations of quarks and gluons evaporated by PBHs [50]), $10^9 \lesssim M_{\rm BH} \lesssim 10^{13}$ g, and from influence of PBH evaporations on the CMB anisotropy, $2.5 \times 10^{13} \lesssim M_{\rm BH} \lesssim 2.5 \times 10^{14}$ g [34], ii) constraints on PBHs from extragalactic photon background, $10^{13} \lesssim M_{\rm BH} \lesssim 10^{17}$ g, iii) constraints on nonevaporating PBHs (gravitational and lensing constraints). Constraints on PBHs from data on extragalactic neutrino background [41,42,51], in the region $10^{11} \lesssim M_{\rm BH} \lesssim 10^{13}$ g, are somewhat weaker than nucleosynthesis constraints.

We do not consider in this paper the PBH constraints from PBH masses smaller than 10^9 g because the corresponding GWB frequencies are too high ($\gtrsim 10^4$ Hz). Also, we did not consider in this paper the constraints from galactic gamma rays (they could be essential in the narrow mass region near $M_{\rm BH} \sim 10^{15}$ g but strongly depend on the unknown clustering factor [34]) and potential constraints [34] from future measurements of 21 cm line.

For a derivation of the constraint on $\mathcal{P}^0_{\mathcal{R}}$ in the region $10^9 \lesssim M_{\rm BH} \lesssim 10^{13}$ g we use the latest update of the nucleosynthesis constraints given in the review [34]. In this region of PBH masses we, following the traditional practice, approximate the initial PBH mass spectrum by δ function (i.e., we assume that all PBHs have the same mass $M_{\rm BH}$). The mass of the PBH formed is approximately equal to the horizon mass at horizon entry, $M_{\rm BH} \approx M_h$. Correspondingly, the constraints are expressed in terms of the function $\beta(M_{\rm BH})$, which is the mass fraction of the energy density of the Universe going to PBHs. It is given by the relation

$$\begin{aligned}\beta(M_{\rm BH}) &= 2\int_{\delta_{\rm th}}^{1} P(\delta_{\rm hor}(R)) d\delta_{\rm hor}(R) \\ &= \mathrm{erfc}\left(\frac{\delta_{\rm th}}{\sqrt{2}\sigma_R(M_{\rm BH})}\right),\end{aligned} \tag{15}$$

where the mass variance is given by [36,42]

$$\sigma_R^2(M_{\rm BH}) = \frac{16}{3}\int_0^\infty (kR)^2 j_1^2\left(\frac{kR}{\sqrt{3}}\right) \exp(-k^2R^2)\mathcal{P}_{\mathcal{R}}(k)\frac{dk}{k}, \tag{16}$$

R is the smoothing scale, i.e., the horizon size.

The order of magnitude of the constraint on β is, according to [34]: $\beta \lesssim 10^{-18}$ for 10^9 g $< M_{\rm BH} < 10^{10}$ g and $\beta \lesssim 10^{-23}$ for 10^{10} g $< M_{\rm BH} < 10^{13}$ g. In the narrow region near $\sim 3 \times 10^{13}$ g there is the strong constraint following from CMB anisotropy damping, $\beta \lesssim 10^{-28}$.

For a derivation of the constraint on $\mathcal{P}^0_{\mathcal{R}}$ in the region $10^{13} \lesssim M_{\rm BH} \lesssim 10^{17}$ g we use the extended PBH mass spectrum given in Sec. II and the technique developed by authors in [42] [in particular, the condition that photons (primary as well as secondary ones [52]) evaporated from PBHs do not exceed the observed extragalactic gamma ray background was used]. Our method is essentially the same as used in the pioneering work [53]. Extragalactic photon background data which we used had been obtained in [54] (EGRET collaboration) and in [55] (Fermi LAT Collaboration). Comparison shows that in the energy region $\sim 0.1 \div 1$ GeV (which is of interest for us) data of both works are consistent with each other. So, for concrete calculations we used the data from [54].

At last, the gravitational constraint is just a condition that $\Omega_{\rm PBH}$ does not exceed the energy density of nonbaryonic dark matter (in the limiting case, PBHs account for all dark matter):

$$\Omega_{\rm PBH} \le \Omega_{\rm CDM} \approx 0.25. \tag{17}$$

The value of $\mathcal{P}^0_{\mathcal{R}}$ is obtained from (14) and (17).

Lensing constraints arise due to the fact that microlensing observations of stars in the Magellanic Clouds probe the fraction of the Galactic halo in massive compact halo objects (MACHOs) of subsolar masses [56]. The fraction of the halo in PBHs is

$$f(M_{\rm BH}) = \frac{\Omega_{\rm PBH}}{\Omega_{\rm CDM}}. \quad (18)$$

From the analysis of MACHO [57] and EROS [58] microlensing surveys, $f(M_{\rm BH}) < 0.1$ for $10^{-6}M_\odot < M_{\rm BH} < M_\odot$ and $f(M_{\rm BH}) < 0.04$ for $10^{-3}M_\odot < M_{\rm BH} < 0.1M_\odot$. There are some additional constraints on $f(M_{\rm BH})$ for other mass ranges, reviewed, e.g., in [34], but they are generally rather weak ($f(M_{\rm BH}) \approx 1$) and we do not use them here.

The resulting constraints are shown in Fig. 2. The constraints based on the $\beta(M_{\rm BH})$ function are designated by thin lines (the corresponding constraints on β have been taken from Fig. 6 of [34]). The constraints obtained by using our technique (which is briefly explained is Sec. II) and EGRET data and gravitational constraints are shown by thick lines. For calculations of limits on $\Omega_{\rm GW}$ in the following Sections we use, for smaller masses (before the crossing points of thin and thick lines), the "β constraint" and for larger masses, after the crossing points, the constraints given by the thick lines. The value of the crossing point is about 4×10^{13} g, almost independently on the value of Σ.

One can see from Fig. 2 that the results for $\mathcal{P}^0_{\mathcal{R}}$ constraint depend on the method of the calculation, in the region $\sim 10^{14} \div 10^{17}$ g. Namely, the constraints based on the β function are somewhat weaker. We did not study, in the present work, the dependence of this result on the form of the PBH mass spectrum.

The $\mathcal{P}^0_{\mathcal{R}}$ constraints shown in Fig. 2 (for the cases of $\Sigma = 3, 5$) are close to the ones derived in [36]. Authors of [36] have assumed that the power spectrum is scale invariant over the (relatively small) range of scales which contribute to a given constraint (this is analogous to the assumption that primordial spectrum has a rather wide peak). They argued that deviations from scale invariance (which are consistent with a slow-roll inflation hypothesis) lead to small changes in the constraints. However, in the case of a narrow peak (our case of $\Sigma = 1$), which can be produced, e.g., by a violent slow-roll violation during single-field inflation, the limit on $\mathcal{P}^0_{\mathcal{R}}$ will, of course, be much weaker, as we see from Fig. 2 (because the total power contained in the spectrum depends on its width).

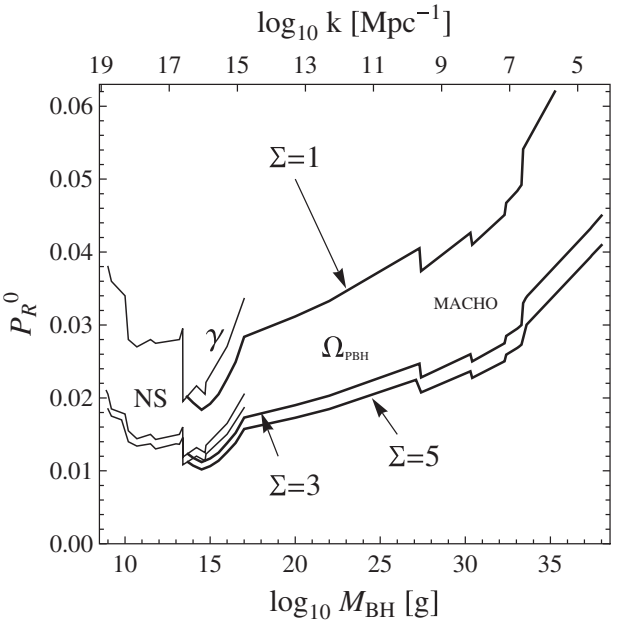

FIG. 2. The limits on the value of $\mathcal{P}^0_{\mathcal{R}}$ from PBH nonobservation for three different values of Σ. The constraints based on the β-function approach are shown by thin lines.

V. INDUCED GW BACKGROUND

A. Basic formulas

According to [6], the power spectrum of induced GWs is given by the expression

$$\mathcal{P}_h(k,\tau) = \int_0^\infty d\tilde{k} \int_{-1}^1 d\mu \, \mathcal{P}_\Psi(|\mathbf{k}-\tilde{\mathbf{k}}|)\mathcal{P}_\Psi(\tilde{k})\mathcal{F}(k,\tilde{k},\mu,\tau), \quad (19)$$

where

$$\mathcal{F}(k,\tilde{k},\mu,\tau) = \frac{(1-\mu^2)^2}{a^2(\tau)} \frac{k^3\tilde{k}^3}{|\mathbf{k}-\tilde{\mathbf{k}}|^3} \times \int_{\tau_0}^\tau d\tilde{\tau}_1 a(\tilde{\tau}_1) g_k(\tau,\tilde{\tau}_1) f(\mathbf{k},\tilde{\mathbf{k}},\tilde{\tau}_1) \times \int_{\tau_0}^\tau d\tilde{\tau}_2 a(\tilde{\tau}_2) g_k(\tau,\tilde{\tau}_2) [f(\mathbf{k},\tilde{\mathbf{k}},\tilde{\tau}_2) + f(\mathbf{k},\mathbf{k}-\tilde{\mathbf{k}},\tilde{\tau}_2)] \quad (20)$$

and

$$f(\mathbf{k},\tilde{\mathbf{k}},\tau) = 12\Psi(\tilde{k}\tau)\Psi(|\mathbf{k}-\tilde{\mathbf{k}}|\tau) + 8\tau\Psi(\tilde{k}\tau)\Psi'(|\mathbf{k}-\tilde{\mathbf{k}}|\tau) + 4\tau^2\Psi'(\tilde{k}\tau)\Psi'(|\mathbf{k}-\tilde{\mathbf{k}}|\tau). \quad (21)$$

In Eqs. (19)–(21) the following notations are used. $\mathcal{P}_\Psi(k)$ is the power spectrum of the Bardeen potential, defined at some moment of time $\tau = \tau_i'$ near the beginning of the RD stage (by definition, it is the primordial spectrum),

$$\langle \Psi_{\mathbf{k}} \Psi_{\mathbf{k}'} \rangle = \frac{2\pi^2}{k^3} \delta^3(\mathbf{k}+\mathbf{k}') \mathcal{P}_\Psi(k), \quad (22)$$

$\Psi_{\mathbf{k}}$ is the Fourier component of Ψ,

$$\Psi(\mathbf{x}) = \frac{1}{(2\pi)^{3/2}} \int d^3\mathbf{k} \Psi_{\mathbf{k}} e^{i\mathbf{k}\cdot\mathbf{x}}, \quad (23)$$

$\mu = \mathbf{k}\cdot\tilde{\mathbf{k}}/(k\tilde{k})$ is the cosine of the angle between the vectors $\mathbf{k}$ and $\tilde{\mathbf{k}}$. The power spectrum of GWs is defined by the standard expression

$$\langle h_{\mathbf{k}}(\tau) h_{\mathbf{k}'}(\tau) \rangle = \frac{1}{2} \frac{2\pi^2}{k^3} \delta^3(\mathbf{k}+\mathbf{k}') \mathcal{P}_h(k,\tau), \quad (24)$$

where $h_{\mathbf{k}}(\tau)$ is the Fourier component of the tensor metric perturbation,

$$h_{ij}(x,\tau) = \int \frac{d^3\mathbf{k}}{(2\pi)^{3/2}} e^{i\mathbf{k}\cdot\mathbf{x}}[h_{\mathbf{k}}(\tau)e_{ij}(\mathbf{k}) + \bar{h}_{\mathbf{k}}(\tau)\bar{e}_{ij}(\mathbf{k})], \tag{25}$$

$e_{ij}(\mathbf{k})$ and $\bar{e}_{ij}(\mathbf{k})$ are two polarization tensors corresponding to the wave number $\mathbf{k}$.

The function f in Eq. (21) contains transfer functions $\Psi(k\tau)$, which are defined by

$$\Psi(k\tau) = \frac{\Psi_k(\tau)}{\Psi_k}, \tag{26}$$

where $\Psi_k \equiv \Psi_k(\tau_i')$ is the initial (primordial) value of the potential. During radiation dominated (RD) epoch, the solution for the Bardeen potential, having the initial condition $\Psi_k(\tau_i) = 0$, where τ_i is the moment of the end of inflation which is close to τ_i' (but $\tau_i < \tau_i'$), is given by Eq. (8). The value of the potential at τ_i is chosen to be zero because Ψ_k is typically very small during inflation [43] and it is a continuous function during the transition from inflationary to RD stage (we assume, for simplicity, that the reheating is instant). We have chosen, for the numerical calculation, the value of τ_i' using the condition $\lg(\tau_i'/\tau_i) = 0.05$ and thereby neglect the formation of PBHs and induced GWs in the interval of time from τ_i to τ_i'. In this work, we are interested only in wave numbers $k \ll k_{\rm end}$, for which there is no dependence of the results on τ_i (because the perturbation amplitudes, such as $\Psi_k(\tau)$, have enough time to reach their asymptotic limit before horizon reentry for each mode). For an example of the case where values of $k \sim k_{\rm end}$ are important, see, e.g., Ref. [42] (where the case of the running mass model is considered).

The function $g_k(\tau,\tilde{\tau})$ in Eq. (20) is the Green function which depends on the cosmological epoch. For RD Universe,

$$g_k(\tau,\tilde{\tau}) = \frac{1}{k}\sin[k(\tau-\tilde{\tau})], \qquad \tau < \tau_{\rm eq}. \tag{27}$$

The energy density of GWs per logarithmic interval of k in units of the critical density is given by

$$\Omega_{\rm GW}(k,\tau) = \frac{1}{12}\left(\frac{k}{a(\tau)H(\tau)}\right)^2 \mathcal{P}_h(k,\tau). \tag{28}$$

Here, the power spectrum of GWs, $\mathcal{P}_h(k,\tau)$, is obtained from the formula (19). However, for very large wave numbers k which we are interested in, the direct use of (19) will require numerical integration for functions having a huge number of oscillations (e.g., for $k \sim 10^{16}$ Mpc^{-1} this is about $\sim k\tau_0 \sim 10^{20}$ oscillations). This is hard to do numerically. Fortunately, we do not have to do integration until the present day. As discussed in [9], it is enough to calculate $\Omega_{\rm GW}$ for the moment of time $\tau_{\rm calc} \gg k^{-1}$ at which the mode is well inside the horizon and is freely propagating. We can then easily relate energy densities of GWs at different times with simple calculation, using the fact that $h_k \sim a^{-1}$ far inside the horizon (this approach works well only for rather large values of k, $k \gtrsim k_c \approx 100k_{\rm eq} \approx 1$ Mpc^{-1}, but we are only interested in such large wave numbers here).

The final expression for $\Omega^0_{\rm GW}(k)$ is [9]

$$\Omega^0_{\rm GW}(k) = 2\Omega_R\left(\frac{g_{*\rm eq}}{g_{*\rm calc}}\right)^{1/3} \times \frac{(k\tau_{\rm calc})^2}{12}\mathcal{P}_h(k,\tau_{\rm calc}). \tag{29}$$

This formula gives the correct energy density, accurate to the oscillations in it. In practice, $\tau_{\rm calc}$ can be either fixed or dependent on k, e.g., for the last case,

$$\tau_{\rm calc} = N_{\rm sub}\cdot k^{-1},\ N_{\rm sub} \sim 100. \tag{30}$$

It proves to be more convenient to use the ''randomized'' value of $N_{\rm sub}$, i.e.,

$$\tau_{\rm calc} = (\tilde{N}_{\rm sub} + N_{\rm rnd})\cdot k^{-1}, \tag{31}$$

where $\tilde{N}_{\rm sub}$ is constant and $N_{\rm rnd}$ is a random number in the interval $[0, 2\pi]$ calculated independently for every k. In this case, the result of the calculation is a stochastically oscillating function whose envelope always can be easily found, and it is the envelope that we are interested in. The exact shape of the function will, actually, depend on the choice of $\tau_{\rm calc} \gg k^{-1}$, and, the larger $\tau_{\rm calc}$ we take, the more frequent are the oscillations, but the envelope which we are interested in does not change. This was explicitly shown in work [9] (see, in particular, Figure 2 from it, which shows the same GW spectrum calculated using approach of Eq. (31) and the one using $\tau_{\rm calc} = $ const. It is seen from that figure that the resulting spectrum is the same).

B. Connection between frequency and horizon mass

For a wave with comoving wave number k and wavelength $\lambda = 2\pi/k$, propagating at the speed of light c, the corresponding frequency is $f = c/\lambda$, or

$$f = \frac{ck}{2\pi} = 1.54\times 10^{-15}\left(\frac{k}{\rm Mpc^{-1}}\right)\ {\rm Hz}. \tag{32}$$

From the constancy of the entropy in the comoving volume, we have the relation between the scale factor a, temperature T, and the effective number of degrees of freedom g_*:

$$a \sim g_*^{-1/3}T^{-1}. \tag{33}$$

From the Friedmann equation ($H^2 \sim \rho$), we have

$$H \sim a^{-2}g_*^{-1/6}, \tag{34}$$

and the horizon mass corresponding to the scale factor a evolves during the RD epoch as

$$M_h \sim (H^{-1})^3\rho \sim a^2 g_*^{1/6}. \tag{35}$$

From (34) and (35), the wave number of the mode entering horizon at the moment of time t (at this time, $k = aH$) is related to the horizon mass at the same moment of time by

$$k = k_{\rm eq}\left(\frac{M_h}{M_{\rm eq}}\right)^{-1/2}\left(\frac{g_*}{g_{*\rm eq}}\right)^{-1/12} \approx 2\times 10^{23}(M_h[\rm g])^{-1/2}\ \rm Mpc^{-1}, \quad (36)$$

where in the last equality we have adopted that $g_{*\rm eq} \approx 3$, $g_* \approx 100$,

$$M_{\rm eq} = 1.3\times 10^{49}\ \rm g\cdot(\Omega_m h^2)^{-2} \approx 8\times 10^{50}\ \rm g, \quad (37)$$

$$k_{\rm eq} = a_{\rm eq}H_{\rm eq} = \sqrt{2}H_0\Omega_m\Omega_R^{-1/2} \approx 0.0095\ \rm Mpc^{-1}. \quad (38)$$

The factor g_* is a function of cosmic temperature T, and in this work we assume that there are no degrees of freedom beyond the standard model, so $g_* \approx 100$ for $T \gtrsim 100$ MeV, $g_* \approx 10$ for 100 MeV $\gtrsim T \gtrsim 1$ MeV and $g_* \approx g_{*\rm eq} \approx 3$ for $T \lesssim 1$ MeV. The connection between horizon mass and T is

$$M_h \approx 3\times 10^5 M_\odot\left(\frac{g_*}{g_{*\rm eq}}\right)^{-1/2}\left(\frac{T}{1\ \rm MeV}\right)^{-2}, \quad (39)$$

and we can estimate that $M_h(1\ \rm MeV) \approx 10^5 M_\odot$, and $M_h(100\ \rm MeV) \approx 5M_\odot$.

The frequency of the wave corresponding to the wave number k can be related to the horizon mass by the relation following from (32) and (36),

$$f \approx 3\times 10^8\ \rm Hz\times(M_h[g])^{-1/2}; \qquad M_h \approx \frac{9\times 10^{16}\ \rm g}{(f[\rm Hz])^2}. \quad (40)$$

For scalar-induced GWs, the single mode in scalar spectrum does not correspond to the only one mode in $\mathcal{P}_h$. For example, for the δ-function-like spectrum $\mathcal{P}_\mathcal{R}(k) \sim \delta(k-k_0)$, the GW spectrum is continuous and stretches from 0 to $2k_0$ [5]. However, the order of magnitude of wave numbers of induced GWs is the same as of scalar perturbations, so (40) gives an estimate of GW frequency that will be generated from perturbations entering horizon at its mass scale M_h. Furthermore, if PBHs form from a scalar spectrum of perturbations at a horizon mass scale M_h, the typical PBH mass will be of order of M_h, so (40) relates the typical PBH mass with the characteristic frequency of second-order GWs produced.

VI. CONSTRAINTS ON $\Omega_{\rm GW}$ FROM PBHS

In Fig. 3, we show the result of $\Omega_{\rm GW}$ calculation for the finite-width distribution of the form (13). It is seen that for a narrow peak, the distribution looks much like the double-peaked one produced by a δ-function power spectrum [5,9]. The shape is smoothing with the growth of Σ (and it will be a scale-invariant spectrum for the scale-invariant input [6]). The value of $\Omega_{\rm GW}$ in the case of rather wide peak ($\Sigma \gg 1$) is proportional to $(\mathcal{P}_\mathcal{R})^2$ and can be estimated as

$$\Omega_{\rm GW}(k > k_c, \tau_0) \cong 0.002\left(\frac{g_{*\rm eq}}{g_*}\right)^{1/3}\cdot\mathcal{P}_\mathcal{R}^2. \quad (41)$$

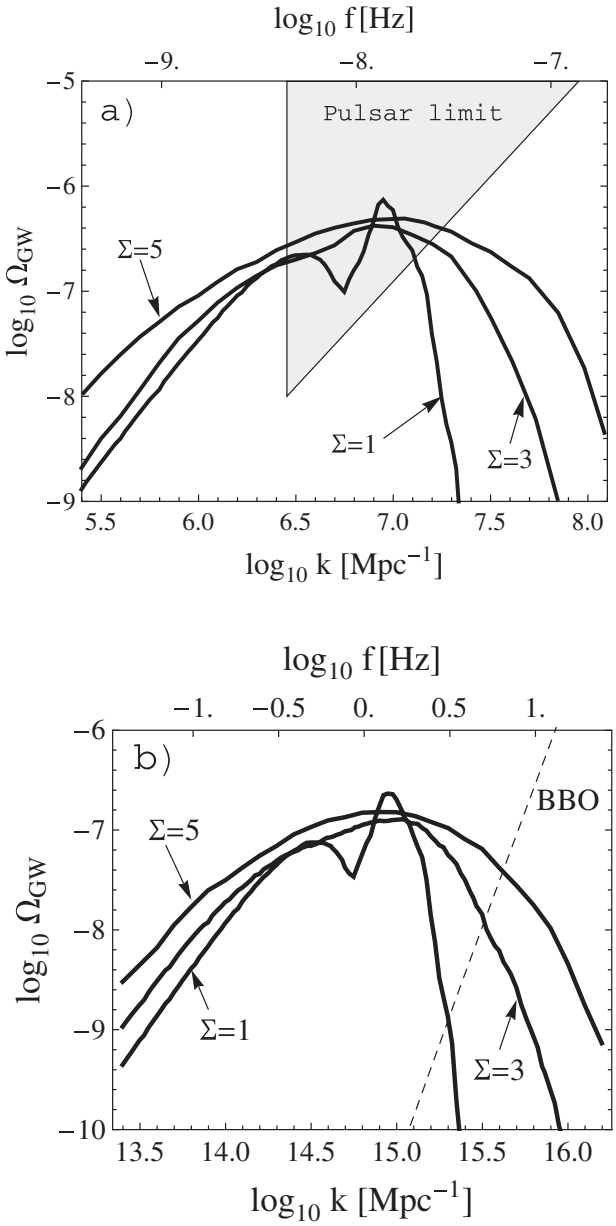

FIG. 3. (a) The calculation of the induced GWB corresponding to primordial power spectra and PBH mass spectra given in Fig. 1 (cases of $\Sigma = 1, 3, 5$). The pulsar timing limit for $\Omega_{\rm GW}$ is also shown. (b) The calculation of the induced GWB for $M_h^0 = 10^{17}$ g (for all three cases, $\Omega_{\rm PBH} \approx 0.24$, the corresponding sets of parameters are $\mathcal{P}_\mathcal{R}^0 = 0.028$ for $\Sigma = 1$, $\mathcal{P}_\mathcal{R}^0 = 0.0172$ for $\Sigma = 3$, and $\mathcal{P}_\mathcal{R}^0 = 0.0159$ for $\Sigma = 5$).

It is seen from Fig. 3 that the maximal values of second-order GWB amplitudes that can be reached do not depend significantly on the width of the primordial power spectrum. The growth of $\Omega_{\rm GW}$ with increase of Σ, which is naturally expected (see [9]), is partly compensated by the simultaneous decrease of the curvature perturbation amplitude $\mathcal{P}_\mathcal{R}^0$ (really, Fig. 2 shows that constraint on $\mathcal{P}_\mathcal{R}$ decreases with the growth of Σ). This allows to put a constraint on the value of $\Omega_{\rm GW}$, which is independent on

the width. Such constraint is shown in Fig. 4 for the whole range of GW frequencies considered, $\sim 10^{-10} \div 10^{4}$ Hz.

The shaded triangle in Figs. 3(a) and 4 designates the pulsar timing limit obtained in [59],

$$\Omega_{\rm GW}(f)h^2 < 4.8 \times 10^{-9}\left(\frac{f}{4.4 \times 10^{-9}\ {\rm Hz}}\right)^2, \qquad (42)$$

for $f > 4.4 \times 10^{-9}$ Hz at 90% C.L. It is seen that PBH mass spectra from Fig. 1 ($M_h^0 = 0.5M_\odot$) are inconsistent with this limit: the same scalar perturbation spectrum overproduces GWs. We have estimated that the limit (42) excludes the significant amount of PBHs in the region of masses $\sim(0.03 \div 10)M_\odot$ due to overproduction of second-order GWs. Note that this conclusion differs from the earlier result of [7] who associate the pulsar timing limit (42) with PBHs of mass $\sim 10^3 M_\odot$. This is obviously caused by the definition $f \equiv 2\pi ck$ used by these authors, instead of the usual one given by Eq. (32). From our results it follows that the primordial origin of intermediate mass black holes (IMBHs), with masses $\sim(10^2$–$10^4)M_\odot$, is not excluded by pulsar timing limits.

PBHs with mass close to $\approx 10^{17}$ g can be responsible for cosmic dark matter, and, as shown in [42,60], if they are clustered in the Galactic center, they can explain the 511 keV photon line observed from its direction (such photons, in this case, are produced by the annihilation of positrons evaporated from PBHs [61,62]). It is seen, in particular, from Fig. 3(b) that to explain this phenomenon with clustered PBHs, $\Omega_{\rm GW}$ must be approaching a value of $\approx 10^{-7}$ near $f \approx 1$ Hz. This region will be probed in future by BBO experiment.

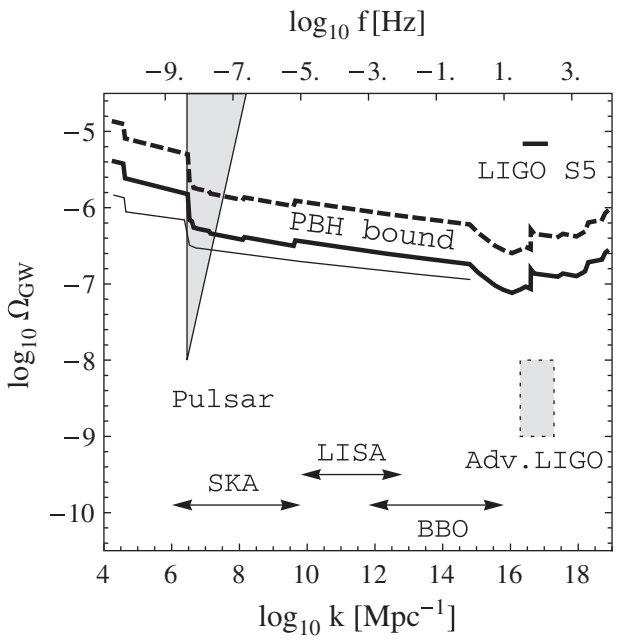

FIG. 4. The limits on the second-order GWB from primordial black holes obtained in this paper. Solid thin line shows the result assuming PBH formation threshold is $\delta_{\rm th} = 1/3$. Dashed line corresponds to the assumption $\delta_{\rm th} = 0.45$. Thin line shows the maximum values of GWB that can be reached for $\Omega_{\rm PBH} = 10^{-5}$ (and $\delta_{\rm th} = 1/3$). Also shown are current pulsar timing limit, LIGO S5 limit, Advanced LIGO planned sensitivity to $\Omega_{\rm GW}$, and frequency ranges in which other future experiments (LISA, BBO, SKA) will operate. The estimate sensitivity of all future experiments, in the corresponding frequency ranges, is much better than the PBH bound shown.

Currently, the analysis of pulsar timing data is the only experiment which allows to set a stronger bound on primordial spectrum than PBHs (see also [63]). For comparison we have also shown the limit obtained by the ground-based interferometer LIGO during its fifth science run (S5) [64],

$$\Omega_{\rm GW} < 6.9 \times 10^{-6}. \qquad (43)$$

This limit applies to a scale-invariant GW spectrum in the frequency range 41.5–169.25 Hz. The target sensitivity [65] of the planned Advanced LIGO experiment, $\Omega_{\rm GW} \sim 10^{-8} \div 10^{-9}$, is also shown in Fig. 4. It is seen that in future the obtained limit for GWB will be experimentally approached in this experiment and also, in most other regions of the frequency range considered, by other experiments such as LISA [66], Big Bang Observer (BBO, see, e.g., [67]), Square-Kilometer-Array (SKA, see, e.g., [68]).

To show the uncertainty in PBH constraints, we have also plotted in Fig. 4 the resulting constraints obtained assuming a somewhat larger PBH formation threshold, $\delta_{\rm th} = 0.45$, and maximal GWB corresponding to $\Omega_{\rm PBH} = 10^{-5}$ (and $\delta_{\rm th} = 1/3$).

VII. SUMMARY AND DISCUSSION

We have performed calculations assuming that PBHs and second-order GWs are produced at times not very close to the beginning of the radiation era t_i. If production of GWs and PBHs takes place near t_i (i.e., right after the end of inflation), the limits derived in our paper can potentially be altered. One such example is a particular case of the running mass inflation model [proposed in [69,70] and further studied in many papers (see [31] and references therein)], which predicts a rather strong scale dependence of the spectral index, possibly leading to largest values of $\mathcal{P}_{\mathcal{R}}(k)$ just near $k_i (\approx k_{\rm end})$. The analysis performed in [9], however, shows that the maximum values of GWB amplitude that can be reached in this case are also very close to maximum values derived in this paper.

In summary, we have performed simultaneous calculations of PBH mass spectra and induced GW background, obtaining the constraints on values of $\mathcal{P}_{\mathcal{R}}(k)$ and $\Omega_{\rm GW}(k)$ from known limits on the PBH concentration in various cosmological scale ranges. We have explored the dependence of these limits on the shape of the primordial spectrum (in particular, on its width). It was shown that though constraints on the peak width may significantly depend on

the shape of the spectrum, the maximal possible values of GWB are almost insensitive to it. This allowed us to place quite model-independent limits on induced GWB in the wide frequency range. We have discussed the applicability of currently available experimental data, in particular, pulsar timing limits, to the constraining of PBH abundance. We have shown that the primordial origin of IMBHs is not forbidden by the pulsar timing limits.

Comparing our results with the previous results of [8,36], one can see that our constraints for $\mathcal{P}^0_{\mathcal{R}}$ almost coincide with those of Ref. [36] in cases when the width of the peak in primordial spectrum is large, $\Sigma = 3, 5$ (see Fig. 2); our constraints for Ω_{GW} are systematically weaker than those of Ref. [8]. Also, in our case the dependence of Ω_{GW} constraint on the shape of the primordial spectrum is much smaller than the analogous dependence in Ref. [8].

[1] S. Matarrese, O. Pantano, and D. Saez, Phys. Rev. Lett. **72**, 320 (1994).
[2] S. Matarrese, S. Mollerach, and M. Bruni, Phys. Rev. D **58**, 043504 (1998).
[3] C. Carbone and S. Matarrese, Phys. Rev. D **71**, 043508 (2005).
[4] S. Mollerach, D. Harari, and S. Matarrese, Phys. Rev. D **69**, 063002 (2004).
[5] K. N. Ananda, C. Clarkson, and D. Wands, Phys. Rev. D **75**, 123518 (2007).
[6] D. Baumann, P. J. Steinhardt, K. Takahashi, and K. Ichiki, Phys. Rev. D **76**, 084019 (2007).
[7] R. Saito and J. Yokoyama, Phys. Rev. Lett. **102**, 161101 (2009).
[8] R. Saito and J. Yokoyama, Prog. Theor. Phys. **123**, 867 (2010).
[9] E. Bugaev and P. Klimai, Phys. Rev. D **81**, 023517 (2010).
[10] Ya. B. Zeldovich and I. D. Novikov, Soviet Astronomy A J. **10**, 602 (1967).
[11] S. Hawking, Mon. Not. R. Astron. Soc. **152**, 75 (1971).
[12] B. J. Carr, arXiv:astro-ph/0511743 (to be published).
[13] M. Y. Khlopov, Astron. Astrophys. **10**, 495 (2010).
[14] D. N. Spergel *et al.* (WMAP Collaboration), Astrophys. J. Suppl. Ser. **170**, 377 (2007).
[15] J. Dunkley *et al.* (WMAP Collaboration), Astrophys. J. Suppl. Ser. **180**, 306 (2009).
[16] E. Komatsu *et al.* (WMAP Collaboration), Astrophys. J. Suppl. Ser. **180**, 330 (2009).
[17] L. Hoi and J. M. Cline, Int. J. Mod. Phys. D **18**, 1863 (2009).
[18] A. A. Starobinsky, Pis'ma Zh. Eksp. Teor. Fiz. **42**, 124 (1985); JETP Lett. **42**, 152 (1985).
[19] L. A. Kofman, A. D. Linde, and A. A. Starobinsky, Phys. Lett. B **157**, 361 (1985).
[20] L. A. Kofman and A. D. Linde, Nucl. Phys. B **282**, 555 (1987).
[21] J. Silk and M. S. Turner, Phys. Rev. D **35**, 419 (1987).
[22] L. A. Kofman and D. Y. Pogosian, Phys. Lett. B **214**, 508 (1988).
[23] D. S. Salopek, J. R. Bond, and J. M. Bardeen, Phys. Rev. D **40**, 1753 (1989).
[24] J. Garcia-Bellido, A. D. Linde, and D. Wands, Phys. Rev. D **54**, 6040 (1996).
[25] L. Randall, M. Soljacic, and A. H. Guth, Nucl. Phys. B **472**, 377 (1996).
[26] J. Lesgourgues, Nucl. Phys. B **582**, 593 (2000).
[27] J. A. Adams, G. G. Ross, and S. Sarkar, Nucl. Phys. B **503**, 405 (1997).
[28] M. Yamaguchi, Phys. Rev. D **64**, 063503 (2001).
[29] M. Kawasaki, T. Takayama, M. Yamaguchi, and J. Yokoyama, Phys. Rev. D **74**, 043525 (2006).
[30] R. Saito, J. Yokoyama, and R. Nagata, J. Cosmol. Astropart. Phys. 06 (2008) 024.
[31] E. Bugaev and P. Klimai, Phys. Rev. D **78**, 063515 (2008).
[32] B. J. Carr, Astrophys. J. **201**, 1 (1975).
[33] M. Y. Khlopov and A. G. Polnarev, Phys. Lett. B **97**, 383 (1980); A. G. Polnarev and M. Y. Khlopov, Sov. Astron. **26**, 391 (1983); Sov. Phys. Usp. **28**, 213 (1985).
[34] B. J. Carr, K. Kohri, Y. Sendouda, and J. Yokoyama, Phys. Rev. D **81**, 104019 (2010).
[35] B. J. Carr, J. H. Gilbert, and J. E. Lidsey, Phys. Rev. D **50**, 4853 (1994).
[36] A. S. Josan, A. M. Green, and K. A. Malik, Phys. Rev. D **79**, 103520 (2009).
[37] E. Bugaev and P. Klimai, JETP Lett. **91**, 1 (2010).
[38] W. H. Press and P. Schechter, Astrophys. J. **187**, 425 (1974).
[39] H. I. Kim and C. H. Lee, Phys. Rev. D **54**, 6001 (1996).
[40] H. I. Kim, Phys. Rev. D **62**, 063504 (2000).
[41] E. V. Bugaev and K. V. Konishchev, Phys. Rev. D **65**, 123005 (2002).
[42] E. Bugaev and P. Klimai, Phys. Rev. D **79**, 103511 (2009).
[43] D. H. Lyth, K. A. Malik, M. Sasaki, and I. Zaballa, J. Cosmol. Astropart. Phys. 01 (2006) 011; I. Zaballa, A. M. Green, K. A. Malik, and M. Sasaki, J. Cosmol. Astropart. Phys. 03 (2007) 010.
[44] B. J. Carr and S. W. Hawking, Mon. Not. R. Astron. Soc. **168**, 399 (1974).
[45] J. C. Niemeyer and K. Jedamzik, Phys. Rev. Lett. **80**, 5481 (1998); Phys. Rev. D **59**, 124013 (1999).
[46] I. Musco, J. C. Miller, and A. G. Polnarev, Classical Quantum Gravity **26**, 235001 (2009).
[47] D. N. Page, Phys. Rev. D **13**, 198 (1976).
[48] Ya. B. Zeldovich and A. A. Starobinsky, M. Yu. Khlopov, and V. M. Chechetkin, Sov. Astron. Lett. **3**, 110 (1977).
[49] D. Lindley, Mon. Not. R. Astron. Soc. **193**, 593 (1980).
[50] K. Kohri and J. Yokoyama, Phys. Rev. D **61**, 023501 (1999).
[51] E. V. Bugaev and K. V. Konishchev, Phys. Rev. D **66**, 084004 (2002).
[52] J. H. MacGibbon and B. R. Webber, Phys. Rev. D **41**, 3052 (1990).

[53] D. N. Page and S. W. Hawking, Astrophys. J. **206**, 1 (1976).
[54] A. W. Strong, I. V.Moskalenko, and O. Reimer, Astrophys. J. **613**, 956 (2004).
[55] A. A. Abdo *et al.* (The Fermi LAT collaboration), Phys. Rev. Lett. **104**, 101101 (2010).
[56] B. Paczynski, Astrophys. J. **304**, 1 (1986).
[57] C. Alcock *et al.* (MACHO Collaboration and EROS Collaboration), Astrophys. J. Lett. **499**, L9 (1998).
[58] P. Tisserand *et al.* (EROS-2 Collaboration), Astron. Astrophys. **469**, 387 (2007).
[59] S. E. Thorsett and R. J. Dewey, Phys. Rev. D **53**, 3468 (1996).
[60] C. Bambi, A. D. Dolgov, and A. A. Petrov, Phys. Lett. B **670**, 174 (2008); **681**, 504(E) (2009).
[61] P. N. Okele and M. J. Rees, Astron. Astrophys. **81**, 263 (1980).
[62] P. H. Frampton and T. W. Kephart, Mod. Phys. Lett. A **20**, 1573 (2005).
[63] H. Assadullahi and D. Wands, Phys. Rev. D **81**, 023527 (2010).
[64] B. Abbott *et al.* (The LIGO Scientific Collaboration & The Virgo Collaboration), Nature (London) **460**, 990 (2009).
[65] B. Abbott *et al.* (LIGO Collaboration), Astrophys. J. **659**, 918 (2007).
[66] http://lisa.jpl.nasa.gov.
[67] J. Crowder and N. J. Cornish, Phys. Rev. D **72**, 083005 (2005).
[68] M. Kramer, arXiv:astro-ph/0409020 (to be published).
[69] E. D. Stewart, Phys. Lett. B **391**, 34 (1997).
[70] E. D. Stewart, Phys. Rev. D **56**, 2019 (1997).